RAPID COMMUNICATIONS IN MASS SPECTROMETRY
Rapid Commun. Mass Spectrom. 2005; **19**: 1649–1656
Published online in Wiley InterScience (www.interscience.wiley.com). DOI: 10.1002/rcm.1970

RCM

Quantification of the plant-derived hallucinogen Salvinorin A in conventional and non-conventional biological fluids by gas chromatography/mass spectrometry after *Salvia divinorum* smoking

Simona Pichini[1]*, Sergio Abanades[2,3], Magí Farré[2,3], Manuela Pellegrini[1], Emilia Marchei[1], Roberta Pacifici[1], Rafael de la Torre[2,4] and Piergiorgio Zuccaro[1]

[1]Drug Research and Evaluation Department, Istituto Superiore di Sanità. Rome, Italy
[2]Institut Municipal d'Investigació Mèdica (IMIM), Barcelona, Spain
[3]Universitat Autònoma, Barcelona, Spain
[4]Universitat Pompeu Fabra, Barcelona, Spain

Received 23 February 2005; Revised 12 April 2005; Accepted 12 April 2005

A gas chromatography method with mass spectrometric detection is described for the determination of Salvinorin A, the main active ingredient of the hallucinogenic mint *Salvia divinorum*. The method was validated in plasma, urine, saliva and sweat using 17-α-methyltestosterone as internal standard. The analytes were extracted from biological matrices with chloroform/isopropanol (9:1, v/v). Chromatography was performed on a 5% phenyl methyl silicone capillary column and analytes were determined in the selected ion monitoring mode. The method was validated over the concentration range 0.015–5 μg/mL plasma, urine and saliva and 0.01–5 μg/patch in the case of sweat. Mean recoveries ranged between 77.1 and 92.7% for Salvinorin A in different biological matrices, with precision and accuracy always better than 15%. The method was applied to the analysis of urine, saliva and sweat from two consumers after smoking 75 mg plant leaves to verify the presence of the active ingredient of *S. divinorum* in human biological fluids as a biomarker of plant consumption. Salvinorin A was detected in urine (2.4 and 10.9 ng/mL) and saliva (11.1 and 25.0 ng/mL), but not in sweat patches from consumers. Copyright © 2005 John Wiley & Sons, Ltd.

Salvia divinorum is a member of the mint family that has been used for centuries by the Mazatec people of Oaxaca, Mexico, in traditional medico-religious ceremonies. The plant is known to the Mazatec Indians as 'ska pastora' or 'ska Maria pastora', and more recently as 'magic mint'.[1,2] The abusers primarily consist of young adults and adolescents who frequent 'smart shops' (now spreading in Europe and selling hemp food, dietary supplements, plant extracts with supposed nutritional and health benefits) or internet websites promoting the drug.

At present, in almost all countries, the use of *S. divinorum* is not banned because neither the plant nor or any of its constituents is listed in the controlled substances lists. In summer 2004, the plant and its main active principle, Salvinorin A, were added to Lists of Controlled Illicit Substances in Italy and sales are prohibited in Spain.[3,4] Abusers ingest the plant using various methods of administration. Fresh leaves can be chewed, or brewed and ingested after the preparation of a tea; dried leaves are chewed or smoked.[5] When converted into a liquid extract, *S. divinorum* can also be vaporized and inhaled.[6] Immediately after ingesting the drug, abusers typically experience vivid hallucinations and potent and intense hallucinatory effects, which, differently from other hallucinogens like LSD and PCP, last for up to an hour or less. High doses of the drug can cause unconsciousness and short-term memory loss.

Salvinorin A (Fig. 1), the main active ingredient of *S. divinorum*, was first identified by Ortega and isolated by Valdes in 1982.[7,8] Salvinorin A is a neoclerodane diterpene and appears to be the only known psychoactive terpenoid of *S. divinorum*.[9] It has been reported as a potent, naturally occurring hallucinogen acting as a full agonist on the kappa opioid receptor.[10] To our knowledge, there are only few published descriptions of the effects of *S. divinorum*. Siebert[6] described the pharmacological effects that occurred after chewing herb leaves or by vaporizing and inhaling pure Salvinorin A. Profound hallucinations were experienced 5–10 min after chewing leaves with Salvinorin A concentrations ranging from 0.89–3.70 mg/g dry weight, and 30 s after inhalation of 200–500 μg pure substance. However, pharmacological

*Correspondence to: S. Pichini, Drug Research and Control Department, Istituto Superiore di Sanità', V.le Regina Elena 299, 00161 Rome, Italy.
E-mail: pichini@iss.it
Contract/grant sponsor: Presidenza del Consiglio dei Ministri, Dipartimento Nazionale per le politiche antidroga, and FIS (G03/005).

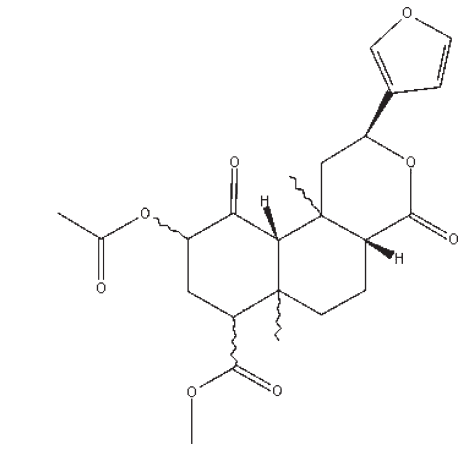

Salvinorin A

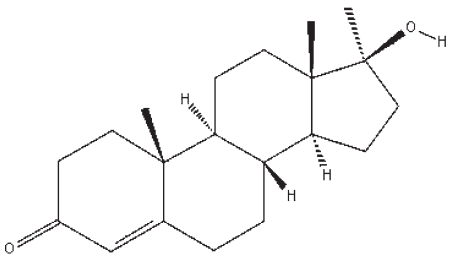

17-α-methyltestosterone (IS)

Figure 1. Chemical structures of Salvinorin A and 17-α-methyltestosterone.

effects were not associated with the presence of the psychoactive Salvinorin A in biological matrices.

This paper reports the development and validation of a sensitive and selective analytical method to determine Salvinorin A in conventional (plasma and urine) and non-conventional (saliva and sweat) biological matrices. The validated method was used to investigate the presence of the active substance in biological fluids of individuals who had consumed dry plant leaves.

EXPERIMENTAL

Materials

The pure standard of Salvinorin A (Fig. 1) was provided as a powder by Prof. Claudio Medana (Department of Analytical Chemistry, Torino University, Torino, Italy). 17-α-Methyltestosterone, which was used as internal standard (IS), was from Sigma (St. Louis, MO, USA). The PharmChek® sweat patches were provided by PharmChem Laboratories (Menlo Park, CA, USA). The patches consisted of a medical-grade cellulose blotter paper collection pad, with an area of 15.4 cm^2, covered by a thin layer of polyurethane and acrylate adhesives. Ultrapure water and all other reagents of analytical grade were obtained from Carlo Erba (Milan, Italy).

Biological samples

Drug-free biological samples (blood, urine, saliva and sweat) were obtained from healthy donors. Blood was immediately centrifuged and the obtained plasma was pooled, aliquoted into 1 mL plastic tubes, and stored at −20°C. Sweat was collected by sweat patches applied to the back of healthy donors, after the skin had been cleaned with a 70% isopropyl alcohol swab, and removed 2 h post-application. Saliva was obtained without any stimulation by spitting into polypropylene tubes; 5 mL of saliva were obtained from each volunteer. Saliva samples were pooled, aliquoted into 1 mL plastic tubes, and stored at −20°C. Different amounts of urine (100–400 mL) were obtained from healthy donors. These samples too were pooled, aliquoted into 1 mL plastic tubes, and stored at −20°C until analysis.

Dry leaves of *S. divinorum* were obtained in a 'Smart Shop' before legal prohibition.

Two subjects with previous experience in the use of hallucinogens (including *Salvia divinorum*) agreed to donate biological samples (urine, saliva and sweat) after smoking dry plant leaves. Saliva samples were collected before and 1 h after *ad lib* smoking 75 mg of dry leaves in a pipe for 3 min. Urine samples were collected at 0–1.5 h and 1.5–9.5 h after smoking. Two sweat patches were applied on the back of the two individuals and removed before (baseline) and 2 h after pipe smoking (when maximal drug recovery was expected taking into account the short duration of the effects). Samples were stored at −20°C until analysis.

Instrumentation

Analyte separation was achieved on a fused-silica capillary column (HP-5MS 30 m × 0.25 mm × 0.25 μm film thickness; Agilent Technologies, Palo Alto, CA, USA). The oven temperature was held at 70°C (for 3 min), raised at 30°C/min to 300°C, and held for 10 min. A splitless injection mode (3 μL) at an injector temperature of 260°C was used. Helium (purity 99%), at a flow rate of 1 mL/min, was the carrier gas.

Gas chromatography/mass spectrometry (GC/MS) analyses were carried out with a Hewlett-Packard (Agilent Technologies, Palo Alto, CA, USA) Series 6890 gas chromatograph equipped with a HP MSD Series mass spectrometer and HP 5973 N Series injector.

The mass spectrometer was operated in EI mode with selected ion monitoring (SIM) acquisition. The ionization was performed at 70 eV, and the ion source and interface temperature were set at 230 and 280°C, respectively. The ions monitored were *m/z* 432, 273 and 94 for Salvinorin A and *m/z* 302, 229 and 124 for the internal standard (IS), 17-α-methyltestosterone. The ions at *m/z* 94 for Salvinorin A and at *m/z* 302 for the IS were selected for the quantification measurement.

Preparation of calibration standards and quality control samples

Stock standard solutions (1 mg/mL) of analytes were prepared in methanol. Working solutions at concentration of 100, 10, and 1 μg/mL were prepared by dilution of the stock standards with methanol and stored at −20°C until analysis. The IS working solution was used at a concentration of 10 μg/mL. Calibration standards containing 0.015 (0.010 for sweat patches), 0.05, 0.1, 0.5, 1.0 and 5.0 μg/mL (or μg/patch) were prepared daily for each analytical batch by adding suitable amounts of methanol solutions to pre-checked drug-free urine, plasma, saliva and sweat patches.

Quality control (QC) samples of 4.25 (high control), 2.0 (medium control) and 0.024 (low control) μg/mL and

μg/patch were prepared in drug-free biological matrices and stored at −20°C. These samples were included in each analytical batch to check calibration, precision, accuracy and stability of samples under storage conditions.

Protocol for preparation of plasma, urine, saliva and sweat patch samples

One mL of urine, serum, saliva and a sweat patch (cut into little pieces) with 50 μL of IS working solution were transferred into 15-mL screw-capped glass tubes and subjected to liquid-liquid extraction with 2 mL of chloroform/isopropanol (9:1). The mixture was homogenized by vortex for 2 min and centrifuged at 2500 rpm for 5 min. The organic layer was transferred to another tube and re-extracted with 2 mL organic mixture. The combined organic layers were evaporated under nitrogen at 40°C. The residue was dissolved in 50 μL ethyl acetate and 3 μL were injected into the GC/MS system.

Validation procedures

Prior to application to real biological samples, the method was tested in a 3-day validation protocol following the accepted criteria for validation of bioanalytical methods. Selectivity, recovery, matrix effect, linearity, precision, accuracy, and limits of detection (LOD) and quantification (LOQ) were evaluated.

Twenty different urine, plasma, saliva samples and ten sweat patches were extracted and analyzed for assessment of potential interferences from endogenous substances. The apparent responses at the retention times of the analyte under investigation and of the IS were compared with the responses of the analyte at the LOQ and of the IS at its lowest quantifiable concentration.

Potential interferences from principal drugs of abuse: opiates (6-monoacetylmorphine, morphine, morphine-3-glucuronide, morphine-6-glucuronide, codeine), cocaine and metabolites (benzoylecgonine and cocaethylene), cannabinoids (delta-9-tetrahydrocannabinol and 11-nor-delta-9-tetrahydrocannabinol-9-carboxylic acid), benzodiazepines (clorazepate, diazepam, lorazepam, oxazepam, alprazolam), and antidepressants (imipramine, clomipramine, fluoxetine, norfluoxetine, paroxetine), also were evaluated by spiking 1 mL of pre-checked drug-free urine, plasma, saliva and a sweat patch with 1 μg of each of the aforementioned substances and carrying out the entire procedure. The potential for carryover was investigated by injecting extracted blank urine, plasma, saliva and sweat patch, with added IS, immediately after analysis of the highest concentration point of the calibration curve on each of the three days of the validation protocol and measuring the areas of the peaks present at the retention times of the analytes under investigation.

Analytical recoveries were calculated by comparing the peak areas obtained when calibration samples were analyzed by adding standard and IS in the extract of drug-free biological matrices tested prior to and after the extraction procedure. The recoveries were assessed at three QC concentration levels, using four replicates at each level.

For an evaluation of matrix effects, the peak areas of extracted blank samples spiked with standards at three QC concentration levels after the extraction procedure were compared with the peak areas of pure diluted substances.

Calibration curves were tested over the 0.015 (0.010 for sweat patches) to 5 μg/mL and μg/patch range for the analytes. Peak area ratios for analyte and IS were used for calculations. A weighted (1/concentration) least-squares regression analysis was used (SPSS, version 9.0.2 for Windows). Five replicates of blank samples were used for calculating the LODs and LOQs. The standard deviation (SD) of the analytical background response was used to determine the detection limit (LOD = 3 SD) and the quantification limit (LOQ = 10 SD). Once calculated, LOQ was tested for acceptance criteria (precision and accuracy coefficient of variation below 20%) and included in calibration curves.

Five replicates at each of three different concentrations of standards (4.25, 2.0, 0.024 μg/mL and μg/patch) added to drug-free samples, extracted as reported above, were analyzed for the determination of intra-assay precision and accuracy. The inter-assay precision and accuracy were determined for three independent experimental assays of the aforementioned replicates. Precision was expressed as the relative standard deviation (RSD) of concentrations calculated for QC samples. Accuracy was expressed as the relative error of the calculated concentrations.

The effect of three freeze/thaw cycles (storage at −20°C) on compound stability in tested biological matrices was evaluated by repeated analysis (n = 3) of QC samples (4.25, 2.0, and 0.024 μg/mL) after each of the three cycles. The stability was expressed as a percentage of the initial concentration of the analyte spiked in tested biological matrices and quantified just after preparation.

RESULTS AND DISCUSSION

Validation results

Representative chromatograms obtained following the extraction of 0.5 μg of Salvinorin A and 17-α-methyltestosterone spiked in 1 mL of drug-free urine, plasma, saliva and in a drug-free sweat patch are shown in Figs. 2 and 3. Since neither deuterated Salvinorin A, nor other terpenoids structurally similar to the tested analyte but not contained in the plant leaves, was available at the time of the study, 17-α-methyltestosterone was chosen as the internal standard (IS). Its physicochemical characteristics and molecular structure are similar to those of Salvinorin A and it is readily available.

Each chromatographic run was completed in 25 min. No additional peaks were observed from any endogenous substances that could have interfered with the detection of the compound of interest. None of the drugs of abuse or aforementioned medications, carried through the entire procedure, interfered with the assay. Blank samples injected after the highest point of the calibration curve did not present any traces of carryover. The recoveries (mean ± SD) for Salvinorin A, obtained after liquid extraction of urine, plasma, saliva and sweat, are shown in Table 1. These results suggested that recoveries from urine samples were the highest, with no relevant differences in extraction recovery for plasma, saliva and sweat patches.

With respect to the matrix effect, the comparison between peak areas of analytes spiked in extracted blank samples and

RCM

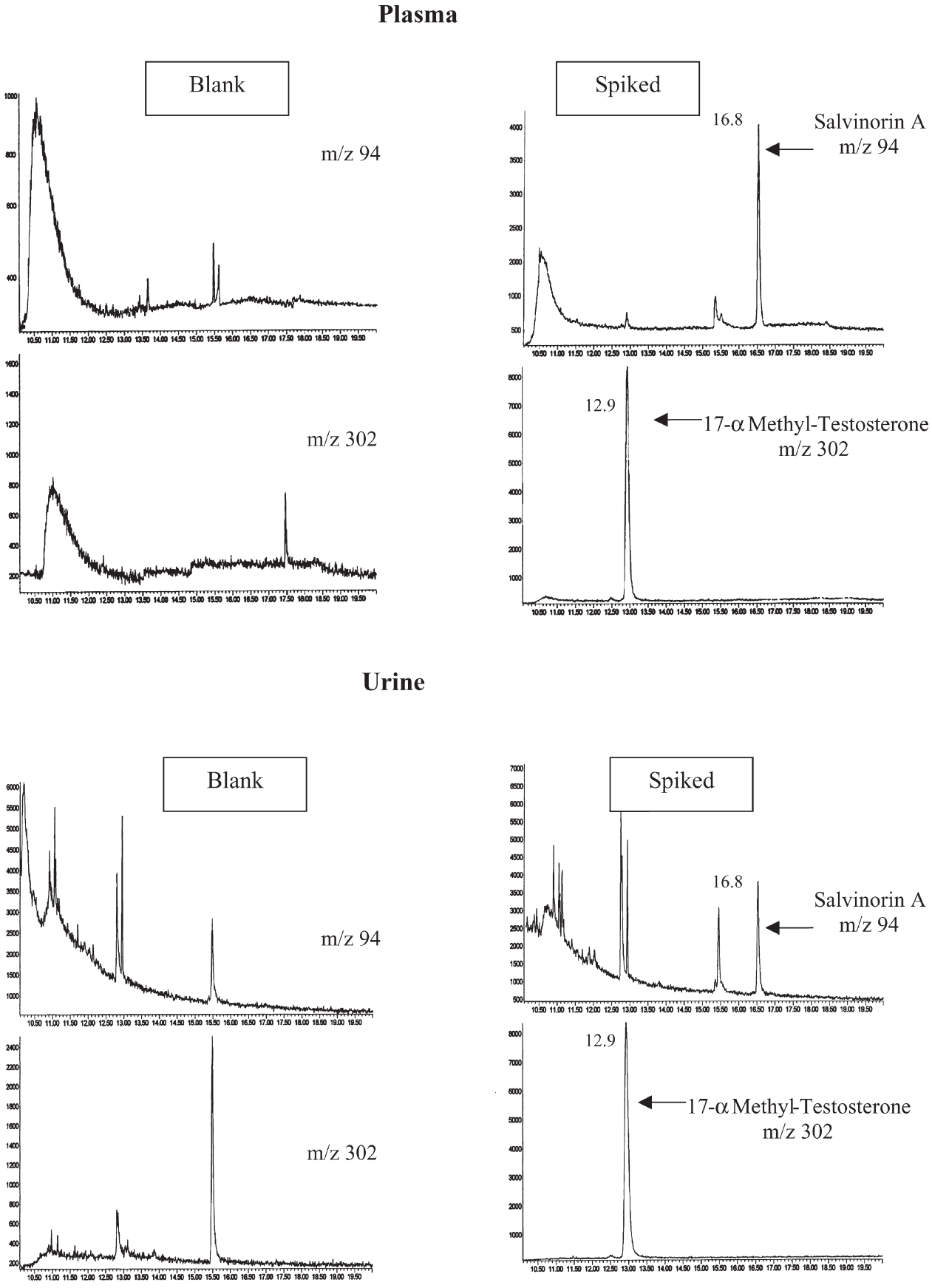

Figure 2. SIM chromatogram of extracts of: 1 mL drug-free plasma sample (left); 1 mL drug-free plasma sample spiked with 0.05 μg Salvinorin A (right), and 1 mL drug-free urine sample (left) with 1 mL drug-free urine sample spiked with 0.05 μg Salvinorin A (right).

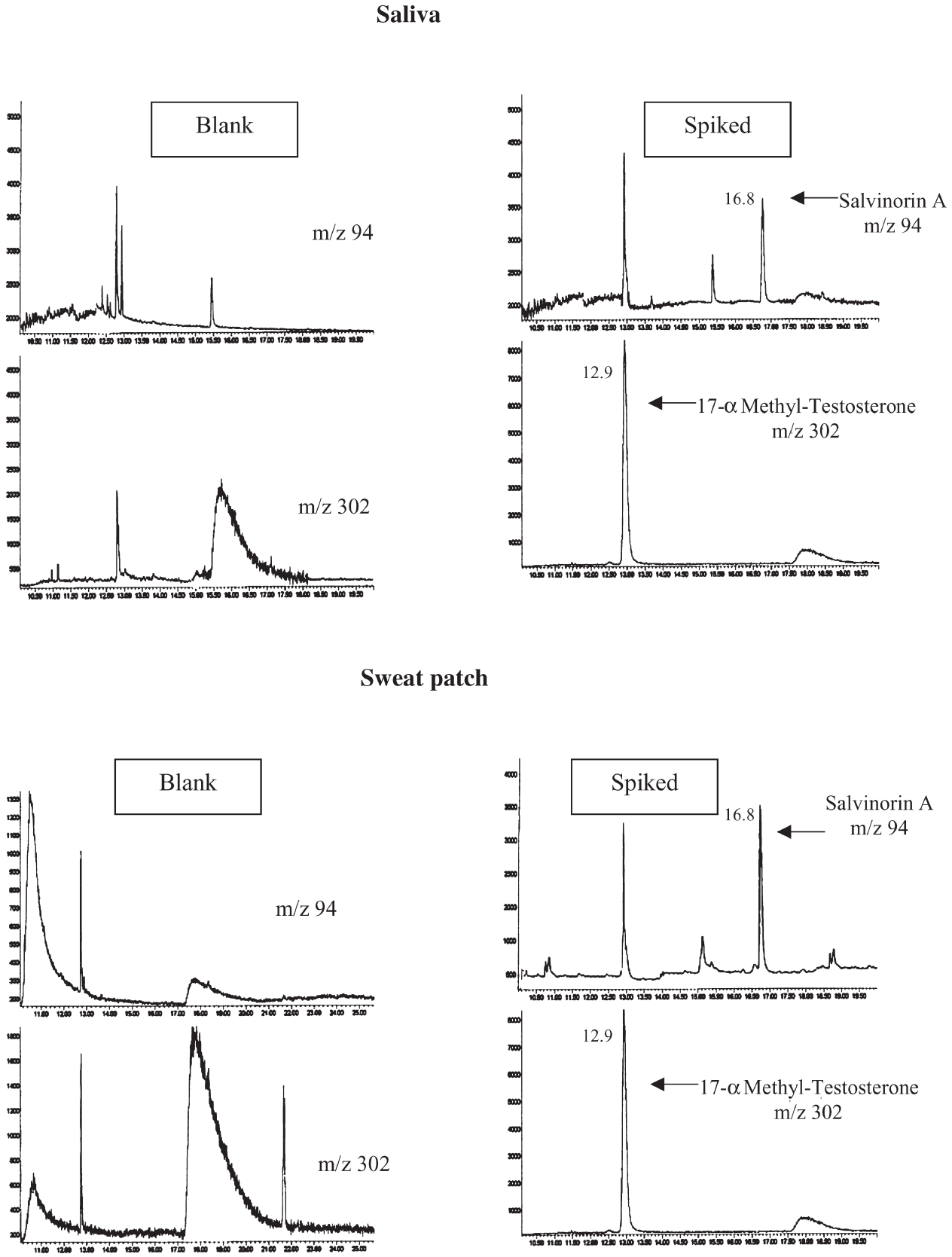

Figure 3. SIM chromatogram of extracts of: 1 mL drug-free saliva sample (left); 1 mL drug-free saliva sample spiked with 0.05 μg Salvinorin A (right), and a drug-free sweat patch sample (left) with sweat patch sample spiked with 0.05 μg Salvinorin A (right).

Table 1. Method calibration in different biological matrices

Biological matrix	Calibration curve slope (n = 3)	Calibration curve intercept (n = 3)	Correlation coefficient (r^2)	LOD (μg/mL)	LOQ (μg/mL)	Recovery (%mean ± SD; n = 4)
Plasma	0.785 ± 0.249	0.042 ± 0.021	0.997 ± 0.003	0.005	0.015	84.6 ± 4.1
Urine	1.192 ± 0.202	0.067 ± 0.012	0.999 ± 0.001	0.005	0.015	93.7 ± 6.7
Saliva	0.721 ± 0.256	0.002 ± 0.015	0.996 ± 0.002	0.005	0.015	84.2 ± 2.4
Sweat*	0.719 ± 0.290	0.016 ± 0.025	0.999 ± 0.002	0.003	0.010	77.1 ± 4.4

* Collected by sweat patches.

Table 2. Intra-day precision and accuracy obtained for Salvinorin A in different biological matrices

Biological matrix	n	Concentration	Estimated mean ± SD	Precision (RSD)	Accuracy (Error %)
		(μg/mL)	(μg/mL)		
Plasma	5	0.024	0.022 ± 0.002	8.6	8.3
	5	0.10	0.091 ± 0.012	13.1	9.0
	5	4.25	3.915 ± 0.198	5.0	7.8
		(μg/mL)	(μg/mL)		
Urine	5	0.024	0.021 ± 0.002	9.5	12.5
	5	0.10	0.097 ± 0.010	10.3	3.0
	5	4.25	3.991 ± 0.210	5.2	8.4
		(μg/mL)	(μg/mL)		
Saliva	5	0.024	0.021 ± 0.002	10.0	12.5
	5	0.10	0.095 ± 0.011	11.5	5.0
	5	4.25	3.895 ± 0.189	4.8	8.3
		(μg/patch)	(μg/patch)		
Sweat	5	0.024	0.022 ± 0.002	10.4	8.3
	5	0.10	0.098 ± 0.010	10.2	2.0
	5	4.25	3.935 ± 0.185	4.7	7.4

those for pure diluted standards showed less than 10% analytical signal suppression due to co-eluting endogenous substances.

The method was linear in the concentration range assayed for all tested biological matrices, with the correlation coefficients (r^2) being higher than 0.99 in all cases. Calibration curve slope values were homogeneous for all the tested biological matrices (t-test with p always >0.05). LODs and LOQs were considered adequate for the purposes of the present study (Table 1).

Tables 2 and 3 show the results obtained for intra-assay and inter-assay precision and accuracy calculations. These results satisfactorily meet internationally established acceptance criteria.[11,12]

With reference to the freeze/thaw stability assays for QC samples, no relevant degradation was observed after three freeze/thaw cycles, with differences from initial concentrations lower than 10%.

Application to analyses of biological samples from plant leaves consumers

This method was used to investigate the presence of Salvinorin A in biological matrices from two volunteers who had smoked dry leaves of *S. divinorum* (Table 4, Fig. 4).

Table 3. Inter-day precision and accuracy for Salvinorin A in different biological matrices obtained for five replicates assayed in three different batches

Biological matrix and compound	n	Concentration	Estimated mean ± SD	Precision (RSD)	Accuracy (Error %)
Plasma		(μg/mL)	(μg/mL)		
Salvinorin A	15	0.024	0.021 ± 0.002	9.5	12.5
	15	0.10	0.095 ± 0.013	13.6	5.0
	15	4.25	3.835 ± 0.199	5.1	9.7
Urine		(μg/mL)	(μg/mL)		
Salvinorin A	15	0.024	0.022 ± 0.002	10.4	8.3
	15	0.10	0.098 ± 0.010	10.2	2.0
	15	4.25	3.935 ± 0.185	4.7	7.4
Saliva		(μg/mL)	(μg/mL)		
Salvinorin A	15	0.024	0.023 ± 0.002	9.1	4.1
	15	0.10	0.099 ± 0.013	13.1	1.0
	15	4.25	3.895 ± 0.189	4.8	8.3
Sweat		(μg/patch)	(μg/patch)		
Salvinorin A	15	0.024	0.021 ± 0.002	10.4	12.5
	15	0.10	0.097 ± 0.014	14.4	3.0
	15	4.25	3.995 ± 0.185	4.6	6.0

Table 4. Salvinorin A concentration in biological fluids from the two subjects after smoking *S. divinorum*

Subject	Dose of Salvinorin A smoked (mg)	Saliva* (ng/mL)	Urine** (ng/mL)		Total amount excreted in urine (ng)		
		1 h post-administration	0–1.5 h	1.5–9.5 h	0–1.5 h	1.5–9.5 h	Sweat patch
A	0.58	25.0	10.9	N.D	7085 (1.2% initial dose)	N.D	N.D
B	0.58	11.1	2.4	N.D	2400 (0.4% initial dose)	N.D	N.D

* Values obtained with 2 mL saliva.
** Values obtained with 10 mL urine.
N.D: not determined.

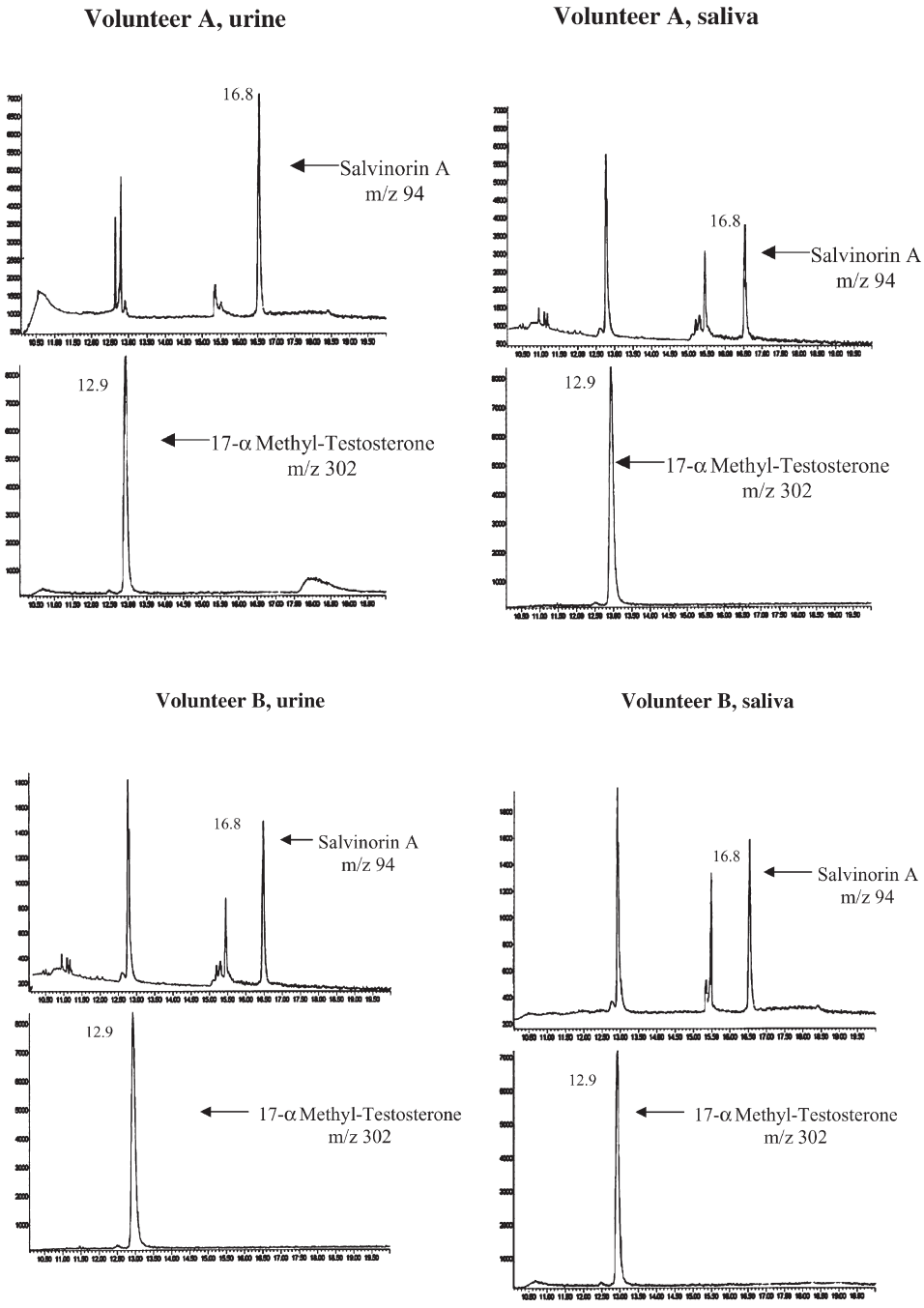

Figure 4. SIM chromatograms of extracts of urine and saliva samples containing 10.9 and 25 ng/mL Salvinorin A, respectively, obtained from two volunteers.

Unfortunately, although the methodology was validated for the different biological matrices that could have been obtained by the two individuals, blood collection was not possible within this experiment. Both volunteers experienced intense hallucinations that started 30 s after inhaling, peaking after 3–5 min, and lasting for about 15–20 min. During that period, blood drawing was considered unsafe and, at the end of the experience, the subjects refused blood collection. Urine, saliva and sweat patch specimens were obtained and Salvinorin A was detected in saliva and urine but not in sweat patches.

Concentrations were in the range of a few ng per mL of biological fluid and saliva (Table 4). Nonetheless, it has to be considered that the amount of consumed preparation (and consequently the amount of the active compound) was extremely low. Indeed, when examining the Salvinorin A content in the dry leaves smoked by the volunteers by a validated methodology,[2] a total amount of 0.58 mg of the active compound (7.7 mg/g dry leaves) was found. Hence, if one accepts the hypothesis that the entire calculated amount was smoked by the two individuals, the concentrations found in saliva and urine samples in the first hour (or hour and half) post-consumption would be in a range compatible with the consumed dose of the drug. The total amount of Salvinorin A excreted in urine represents from 0.4–1.2% of the theoretically administered dose although the true inhaled dose is unknown because one part may have been lost in the combustion and some to sidestream. Salvinorin A was not detected in urine samples collected from 1.5–9.5 h after smoking, probably because of a dilution effect, which yielded concentrations below the LOD obtainable with this methodology. Another possible explanation could be related to fast elimination of the compound, but the pharmacokinetics parameters of Salvinorin A have not been reported. Conversely, regarding the absence of Salvinorin A in sweat patches, previous experience with other drugs of abuse administered as hundred mg doses under controlled conditions and quantified in the range of ng/patch[13–15] led us to conclude that the low amount of administered substance coupled with the small volume of sweat collected in the patch area over such a short wear period resulted in minimal excretion of Salvinorin A.

Nonetheless, sweat was only collected for 2 h after drug administration, while normal sweat patch application involves wearing the patch for 1 week. However, this is normally done to check exposure to illicit drugs in subjects who are not under medical supervision. Thus, the moment of exposure to drugs is not known. This is not the case with controlled drug administration. It seems that Salvinorin A is rapidly absorbed after smoking of dry leaves (maximum effects occur in 3–5 min after consumption), and the fact that it appears only in urine samples collected up to 1.5 h also suggests a rapid elimination (or else an extensive metabolism to unknown substances) and thus a theoretical passage to sweat in the first hours after administration. On the other hand, the non-polar nature of the compound, which does not favor excretion through sweat, and the low concentration of the active principle in the consumed plant leaves are consistent with the lack of detection of this substance in patches worn for 2 h after drug consumption.

CONCLUSIONS

A simple and reliable GC/MS method is reported for the analysis of Salvinorin A in conventional and non-conventional biological matrices. The method was validated according to internationally accepted criteria; it consists of an easy sample preparation by liquid extraction, followed by chromatographic separation on a capillary column and detection in SIM mode. For the first time, the presence of the psychoactive ingredient of *Salvia divinorum*, Salvinorin A, was detected in the urine and saliva of two subjects in the first 1.5 h after its consumption. Pharmacological effects experienced by subjects were intense and short-lived, in agreement with a previous report.[6]

Acknowledgements

This study was supported by Presidenza del Consiglio dei Ministri, Dipartimento Nazionale per le politiche antidroga, and FIS (G03/005).

REFERENCES

1. Valdes LJ. *J. Psychoactive Drugs* 1994; **26**: 277.
2. Giroud C, Felber F, Augsburger M, Horisberger B, Rivier L, Mangin P. *Forensic Sci. Int*. 2000; **112**: 143.
3. Available: www.ministerosalute.it/imgs/C_17_normativa_484_allegato.pdf.
4. Available: www.boe.es (number 32, February 6, 2004).
5. Available: www.sagewisdom.org.
6. Siebert DJ. *J. Ethnopharmacol*. 1994; **43**: 53.
7. Ortega A, Blount JF, Manchand PS. *J. Chem. Soc. Perkin Trans*. 1982; **1**: 2505.
8. Valdes LJ, Butler WM, Hatfield GM, Paul AG, Koreeda M. *J. Org. Chem*. 1984; **49**: 4716.
9. Gruber JW, Siebert DJ, Der Marderosian AH, Hock RS. *Phytochem. Anal*. 1999; **10**: 22.
10. Roth BL, Baner K, Westkaemper R, Siebert D, Rice KC, Steinberg S, Ernsberger P, Rothman RB. *Proc. Natl. Acad. Sci. USA* 2002; **99**: 11934.
11. Guidance for Industry, Bioanalytical Method Validation, US Department of Health and Human Services, Food and Drug Administration, May 2001. Available: http://www.fda.gov/cder/guidance/4252fnl.htm.
12. ICH Topic Q 2 B Validation of Analytical Procedures: Methodology, The European Agency for the Evaluation of Medicinal Products, ICH Technical Coordination: London. Available: http://www.emea.eu.int/htms/human/ich/quality/ichfin.htm.
13. Pichini S, Navarro M, Pacifici R, Zuccaro P, Ortuno J, Farre M, Roset PN, Segura J, de la Torre R. *J. Anal. Toxicol*. 2003; **27**: 294.
14. Saito T, Wtsadik A, Scheidweiler KB, Fortner N, Takeichi S, Huestis MA. *Clin. Chem*. 2004; **50**: 2083.
15. Uemura N, Nath RP, Harkey MR, Henderson GL, Mendelson J, Jones RT. *J. Anal. Toxicol*. 2004; **28**: 253.

Identification of the Molecular Mechanisms by Which the Diterpenoid Salvinorin A Binds to κ-Opioid Receptors†

Feng Yan,[‡,§] Philip D. Mosier,[‡,||] Richard B. Westkaemper,[||] Jeremy Stewart,[⊥] Jordan K. Zjawiony,[⊥] Timothy A. Vortherms,[§] Douglas J. Sheffler,[§] and Bryan L. Roth*[,§,#]

Departments of Biochemistry, Psychiatry, and Neurosciences and Comprehensive Cancer Center, Case Western Reserve University Medical School, Cleveland, Ohio 44106, Department of Medicinal Chemistry, Virginia Commonwealth University, Richmond, Virginia 23284, and Department of Pharmacognosy, University of Mississippi, University, Mississippi 38677

Received March 16, 2005; Revised Manuscript Received May 2, 2005

ABSTRACT: Salvinorin A is a naturally occurring hallucinogenic diterpenoid from the plant *Salvia divinorum* that selectively and potently activates κ-opioid receptors (KORs). Salvinorin A is unique in that it is the only known lipid-like molecule that selectively and potently activates a G-protein coupled receptor (GPCR), which has as its endogenous agonist a peptide; salvinorin A is also the only known non-nitrogenous opioid receptor agonist. In this paper, we identify key residues in KORs responsible for the high binding affinity and agonist efficacy of salvinorin A. Surprisingly, we discovered that salvinorin A was stabilized in the binding pocket by interactions with tyrosine residues in helix 7 (Tyr313 and Tyr320) and helix 2 (Tyr119). Intriguingly, activation of KORs by salvinorin A required interactions with the helix 7 tyrosines Tyr312, Tyr313, and Tyr320 and with Tyr139 in helix 3. In contrast, the prototypical nitrogenous KOR agonist U69593 and the endogenous peptidergic agonist dynorphin A (1−13) showed differential requirements for these three residues for binding and activation. We also employed a novel approach, whereby we examined the effects of cysteine-substitution mutagenesis on the binding of salvinorin A and an analogue with a free sulfhydryl group, 2-thiosalvinorin B. We discovered that residues predicted to be in close proximity, especially Tyr313, to the free thiol of 2-thiosalvinorin B when mutated to Cys showed enhanced affinity for 2-thiosalvinorin B. When these findings are taken together, they imply that the diterpenoid salvinorin A utilizes unique residues within a commonly shared binding pocket to selectively activate KORs.

Salvinorin A (Figure 4) is the major active ingredient of *Salvia divinorum*, a hallucinogenic plant that has been used historically in the traditional shamanic practices of the Mazatec people of Oaxaca, Mexico (*1*−*3*). We recently discovered that salvinorin A, a neutral diterpenoid, activates κ-opioid receptors (KORs)[1] (*4*) and is unique in that it represents the only known lipid-like small molecule that selectively and potently activates a peptidergic G-protein coupled receptor (GPCR) (*5*, *6*). Salvinorin A is highly selective for KOR and has no significant activity at μ, δ, or ORL1-opioid receptors (*4*, *7*) nor other tested GPCRs, neurotransmitter transporters, or ion channels (*4*). Because of its unique structure and selectivity for a single GPCR, the salvinorin A-KOR receptor−ligand complex provides a model system for exploring the molecular and atomic features responsible for small-molecule selectivity among highly homologous receptors. Salvinorin A also provides a tool for further study of the activation mechanisms of GPCRs.

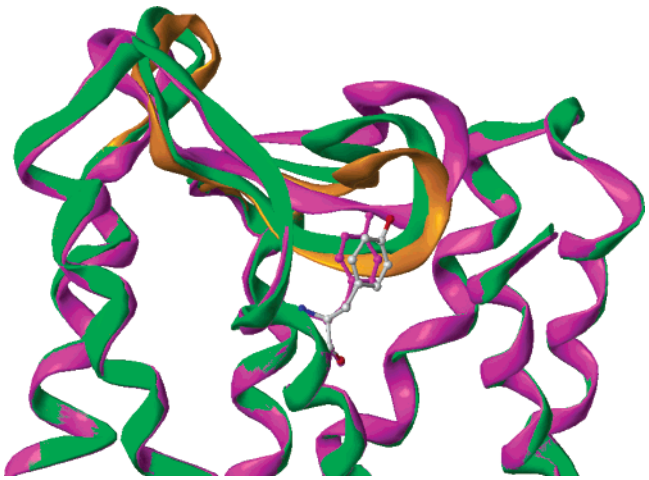

FIGURE 1: Comparison of the e2 loop structures. Comparison of the e2 loop structures from the initial minimized KOR (orange), the MD-averaged and minimized structure (green), and the minimized structure of the MD snapshot taken at 2225 fs (magenta). The position of Tyr313 in TM7 is illustrated.

† This research was supported in part by RO1DA017204, KO2MH01366, and the NIMH Psychoactive Drug Screening Program to B.L.R.

* To whom correspondence should be addressed: Department of Biochemistry, RM W441, School of Medicine, Case Western Reserve University, 2109 Adelbert Road, Cleveland, OH 44106. Telephone: 216-368-2730. Fax: 216-368-3419. E-mail: bryan.roth@case.edu.

‡ These authors contributed equally to this work.

§ Department of Biochemistry, Case Western Reserve University Medical School.

|| Virginia Commonwealth University.

⊥ University of Mississippi.

Departments of Psychiatry and Neurosciences and Comprehensive Cancer Center, Case Western Reserve University Medical School.

[1] Abbreviations: KOR, κ-opioid receptor; GPCR, G-protein coupled receptor.

10.1021/bi050490d CCC: $30.25
Published on Web 05/26/2005

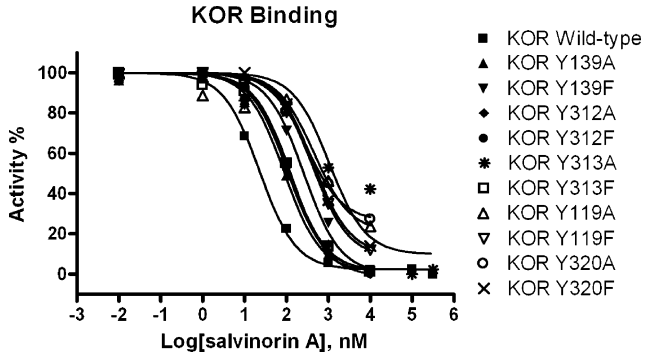

FIGURE 2: Effects of various mutations on salvinorin A binding to KORs reveals the importance of Y313. Shown are representative competition binding isotherms for inhibition of 3H-diprenorphine binding to cloned KORs transiently expressed in HEK-293-T cells. Curves represent the theoretical fits for a single binding site model. K_i values are found in Table 2. For the sake of clarity, error bars are omitted but were typically <10%.

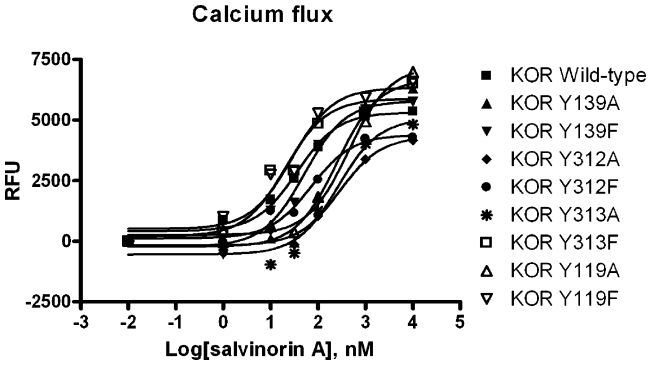

FIGURE 3: Activation of wt and mutant KORs by salvinorin A. Shown are representative dose−response studies for activation of wt and mutant KORs transiently expressed in HEK-293 cells (see the Experimental Procedures for assay details). Curves represent the theoretical fits for the parameter estimates provided in Table 3; for purposes of clarity, error bars are omitted but were typically <10%.

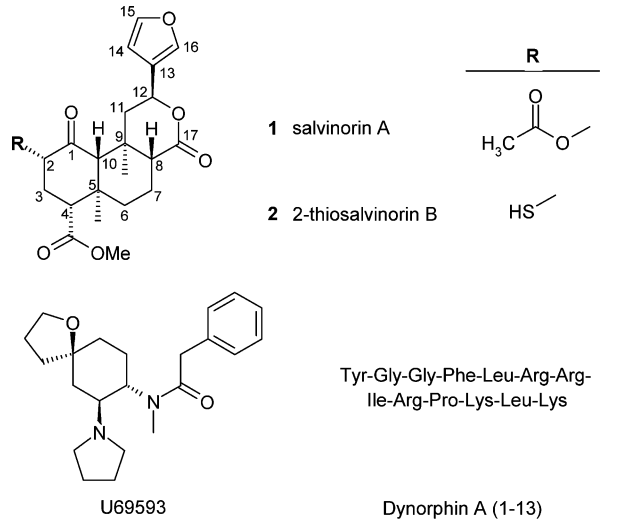

FIGURE 4: Structures of salvinorin A and other compounds used in the current studies.

The binding pocket of the KOR will not be known with certainty until the structure of a KOR−ligand complex is solved. In the absence of direct structural information, combined molecular modeling/mutagenesis studies can provide testable models for ligand interactions and activation mechanisms (*8*−*10*), and we and others have used these approaches with great success for biogenic amine (*9*, *11*) and peptide (*4*, *12*) receptors. Historically, attention has been focused on ionic interactions and hydrogen-bond-type interactions between ligands (either small molecule or peptidergic) and highly conserved charged residues (e.g., Asp and Glu) or residues capable of forming hydrogen bonds (e.g., Tyr and Arg) for anchoring and orienting ligands in the binding pocket (see ref *8* for a review). Because salvinorin A possesses no ionizable groups, ionic interactions cannot provide stability in the binding pocket, although it is conceivable that hydrogen-bond-type interactions could be involved (*4*).

In the current study, we examined the molecular and atomic features essential for the binding and activation of KORs by salvinorin A. Previous computer modeling predicted the key residues that are believed to contribute in salvinorin A binding to KOR: Tyr313, Gln115, Tyr312, and Tyr139 (*4*). To determine if these residues are involved in salvinorin A binding, KOR mutants were constructed and the binding site between salvinorin A and KOR was investigated via radioligand binding and functional and molecular modeling studies. We also employed a novel combined chemical-mutagenesis approach, whereby the effects of cysteine-substitution mutageneses were evaluated for a novel salvinorin A analogue that possesses a free sulfhydryl group.

EXPERIMENTAL PROCEDURES

Materials. Standard reagents, unless stated otherwise, were purchased from Sigma−Aldrich (St. Louis, MO). [^{3}H]-Diprenorphine (K_d = 0.2 nM to KOR; 50 Ci/mmol) was obtained from PerkinElmer−LifeScience Inc. The XL2-Blue *Escherichia coli* strain was purchased from Stratagene (La Jolla, CA). Two sources of salvinorin A were used for the studies described here: Biosearch and the *Salvia divinorum* Research and Information Center, Malibu, CA.

The human KOR cDNA was obtained from the Guthrie Research Foundation (GenBank accession number NM000912) and subcloned into the eukaryotic expression vector pIRESNEO (Invitrogen, Carlsbad, CA). $G_{\alpha 16}$ was obtained from the Guthrie Research Foundation; both constructs were verified by automated dsDNA sequencing (Cleveland Genomics, Inc., Cleveland, OH) before use. A stable line expressing the human KOR (hKOR-293) was obtained by transfecting a hKOR expression vector (hKOR-pIRESNEO) into human embryonic kidney-293 cells and selecting in 600 μg/mL G418. The cells were maintained and transfected as previously detailed (*4*). Surviving clones were expanded and characterized with one (hKOR-293) that expressed high levels of hKOR (ca. 1 pmol/mg) used for further studies.

2-Thiosalvinorin B Synthesis. Salvinorinyl chloride (16 mg, 40 μmol) was placed in DMF (2 mL) containing sodium hydrogen sulfide (6.4 mg, 114 μmol), and the mixture was heated to 35−40 °C for 1 h. Brine water (2 mL) was added, and the mixture was extracted 3 times with ethyl acetate (5 mL). The combined organic extracts were concentrated in vacuo, and the residue was redissolved in acetone (HPLC grade, 1 mL) and separated by HPLC (C_{18} column, MeCN/H_2O 1:1, detection at 210 nm). 2-Thiosalvinorin B (6.9 mg, 44% yield) was collected at R_t = 8.9 min. Complete details

of synthesis and chemical characterization will be reported separately (*13*) (Stewart et al., manuscript in preparation)

Site-Directed Mutagenesis. The mutations were introduced using the Quickchange mutagenesis kit from Stratagene according to the recommendations of the manufacturer. The presence of the mutations was verified by automated dsDNA sequencing (Cleveland Genomics, Inc., Cleveland, OH) before use. Clones expressing high and comparable levels of KOR mutants were studied by radioligand saturation and competition binding experiments as described later.

Radioligand Binding Assays. Radioligand binding assays were preformed as previously detailed (*4*). In brief, crude cell membranes were prepared by lysing transfected HEK-T cells in binding buffer (50 mM Tris-Cl, 10 mM $MgCl_2$, and 0.1 mM EDTA at pH 7.40) and centrifugation at 30000*g* for 20 min. Membrane pellets were then stored at −80 °C until use in binding assays. Binding assays were conducted in total volumes of 0.2 mL in 96-well plates in a binding buffer containing 0.1−0.2 nM ^{3}H-diprenorphine with 10 μM naloxone to determine nonspecific binding for a total of 60 min at room temperature. Assays were terminated by harvesting over GF-C Whatman filters, which had been pre-equilibrated with 0.01% polyethyleneimine and 3 quick washes with ice-cold binding buffer. After the filters had dried, they were counted by liquid scintillation spectrometrometry. K_i determinations were performed by using six concentrations of unlabeled ligand spanning a 10 000-fold dose range. The raw data was analyzed by Prism 4.01 (GraphPad Software, Inc., San Diego, CA) to give K_i values reported as the mean ± standard error of the mean (SEM).

Functional Assays. Functional assays using wild-type and mutant KORs were performed as previously detailed (*14*). Briefly, wild-type and mutant receptors were cotransfected with $G\alpha_{16}$ into HEK-293 cells, and measurements of agonist-induced intracellular Ca^{2+} release were monitored using a Molecular Devices FLEXSTATION II (see ref *15* for details). The raw data were analyzed by Prism 4.01 (GraphPad Software, Inc., San Diego, CA) to give EC_{50} and E_{max} values.

κ-Opioid Receptor Modeling and Ligand Docking. Modeling studies were performed using SYBYL (version 6.9.2, 2004, Tripos Associates, Inc., St. Louis, MO), and a new KOR model was constructed using a rhodopsin template essentially as previously described for the 5-HT_{2A} receptor (*15*). An unambiguous alignment of the rhodopsin and KOR sequences was performed manually by matching the highly conserved residues in transmembrane helices previously identified (*16*, *17*). Because the sequences of the KOR and rhodopsin are similar in length, there are very few insertions (four) and deletions (two) evident in the alignments of the KOR and rhodopsin sequences in the structurally important extra- and intracellular loops; the helical segments contained no insertions or deletions. The COMPOSER module of SYBYL was used to construct an initial model from an experimental bovine rhodopsin structure (A chain of 1F88) (*17*). Amino acid side-chain geometries for the KOR receptor model were established from backbone-dependent libraries of rotamer preference using SCWRL (*18*). The helix backbone geometry of rhodopsin was transferred without change in this procedure. The PROTABLE facility within SYBYL was used to identify sites of unusual and sterically clashing side-chain geometries that were interactively corrected as necessary. Model minimizations were performed using the Tripos Force Field using Gasteiger−Huckel charges with a distance-dependent dielectric constant = 4 and nonbonded cutoff = 8 Å to a gradient of 0.05 kcal/(mol Å).

The KOR model was further modified by minimization with an ensemble of known agonists (bremazocine, morphine, MPCB, U69593, and 6′-GNTI) docked into the receptor. The ensemble of structurally diverse κ agonists was created by successive superimposition of ligands according to previous suggestions based on known structure activity relationships in addition to obvious structural similarities (*19*, *20*). A model of a complex between the antagonist nor-BNI and KOR served as the starting point for subsequent superimpositions. This initial complex was generated by interactive docking of nor-BNI in a fashion consistent with probable interactions with H291, D138, and E297 of the KOR (*21*−*23*).

To explore the inherent flexibility of the e2 loop and the effects of the e2 loop in limiting ligand access to Tyr313, molecular dynamics (MD) simulations were performed. The N terminus of the rhodopsin structure folds over the β turn of the e2 loop. It has been previously shown that the N-terminal region is not necessary for binding to the MOR (*24*, *25*). In addition, there was little similarity in sequence or length between the N termini of rhodopsin and the KOR. Thus, in preparation for the MD simulations, the N terminus of the KOR was removed so as not to constrain the e2 loop during the simulation. The residues deleted included all those up to but not including Pro56. The orientation of the Tyr313 side chain in the original KOR model was directed away from the interior of the receptor (χ_1 = 67.8°). To explore the possibility of direct ligand interaction with Tyr313, its side-chain position was adjusted so that it would be accessible from the interior of the KOR (χ_1 = 275.0°). In its new position, Tyr313 is projected toward and can potentially interact with residues in the e2 loop, including Val205, Asp206, Ile208, and Glu209. An MD simulation was performed for 100 ps using the default settings of the MD routine within SYBYL and maintaining all residues except the e2 loop (Val195−Asp223) as an aggregate to observe the behavior of the loop. The position of the backbone of residues Cys210, Ser211, and Leu212 during the MD run remained close to the interior cavity of the receptor, and their positions in the averaged structure are relatively close to the corresponding backbone atoms in the original KOR. At no time during the simulation did the e2 loop completely exit the interior cavity of the KOR. An average KOR structure was then generated from individual MD conformations and was subsequently energy-minimized. In addition, a snapshot from the MD run at 2225 fs when the loop was farthest from the binding pocket and Glu209 was hydrogen-bonded to Tyr313 was selected and minimized, providing a KOR model with a greater accessibility to Y313 (Figure 1).

GOLD version 2.2 (*26*, *27*) was used to dock salvinorin A and 2-thiosalvinorin B into the MD-averaged and minimized KOR model and into the minimized MD snapshot model. Prior to docking, the CONCORD routine within SYBYL was used to assign initial conformations to salvinorin A and 2-thiosalvinorin B. Several GOLD studies were performed, representing three distinct GOLD configurations. In the first GOLD configuration, standard default settings (no speed-up) for the genetic algorithm (GA) and annealing

Table 1: Residues within Specified Heavy-Atom Distances between the Salvinorin A Ligand and the KOR Receptor for the Proposed Binding Mode[a]

3.0 Å	3.5 Å	4.0 Å	4.5 Å	5.0 Å
none	I135	Y66	M112	Y139
	D138	Y119	A298	P215
	E209	V134		
	C210	S211		
	I294	L212		
	Y313	F214		
	I316	E297		
	Y320	Y312		

[a] Receptor atoms may be part of the backbone or the side chain.

parameters were used and 10 individual GA runs were performed. A large active-site radius of 25.0 Å about the Asp138 γ-carbon atom was used to define the receptor site, thus allowing for the possibility of direct interaction of salvinorin A with distant residues, including Tyr313. In the second GOLD configuration, the GA and annealing parameters corresponding to the 3× speedup option in GOLD were used and 30 individual GA runs were performed. A somewhat more focused 15-Å radius about the Tyr313 side-chain oxygen atom was used to define the receptor site. A third configuration, used only with the minimized MD snapshot at 2225 fs, was identical to the second configuration with the exception that a 20.0-Å radius was used. In each GOLD configuration, cavity detection and ring corner flipping were enabled and the GoldScore scoring function was used to rank the docked solutions. Final docked complexes were evaluated interactively, and ligand rotatable bonds and amino acid residue side-chain torsion angles were scanned manually to estimate the probability that dipolar ligand−side-chain interactions could occur in a stereoelectronically favorable fashion. The complexes were then energy-minimized to identify and resolve any remaining strain within the system. From among all top-ranked docked solutions, one distinct family of docked complexes was selected to represent the dominant binding mode based on its ability to account for all of the observed mutation effects described in this work. The final model was selected from a study representing the third GOLD configuration.

All molecular modeling was carried out on IRIX 6.5-based Silicon Graphics, Inc. workstations.

RESULTS

Radioligand Binding and Functional Parameters of Native and Mutant KORs Reveal Differential Modes of Agonist Binding and Activation. We performed site-directed mutagenesis studies and characterized the binding and functional parameters of the mutated KORs. All of the mutants were expressed at high levels in HEK 293T cells and all had comparable affinity for the antagonist [^{3}H]-diprenorphine (Table 2) and natural agonist dynorphin A (1−13), with the exceptions of the Y139F (8-fold attenuation), Y119F and Y320F (6-fold attenuation each), and Y119A (4-fold attenuation). These results demonstrate that the mutations studied did not significantly alter KOR receptor expression nor significantly perturb the topology of the receptor because binding for the high-affinity antagonist and endogenous agonist dynorphin were not greatly attenuated (e.g., <10-fold change in affinities).

In 4 of 10 of the studied KOR mutants, the affinity for salvinorin A was not significantly altered from wild-type KOR (Table 2). However, a dramatic decrease in the affinity of salvinorin A was obtained by introducing a single mutation, Y313A on TM7 (K_i = 694 nM, 22-fold decrease), a smaller effect was seen for U69369 binding, and no significant effect was seen for dynorphin A (1−13). These results were predicted by our previously published modeling studies (*4*). To elucidate the molecular mechanism(s) responsible for the selective interaction of salvinorin A with Tyr313, we examined a Y313F mutation that should maintain hydrophobic interactions and should abolish hydrogen-bond-type interactions between the −OH of Tyr313 and salvinorin A. Surprisingly, the Y313F mutation caused no loss of the binding affinity, indicating that hydrophobic interactions between salvinorin A and Tyr313 provide stabilization of salvinorin A in the binding pocket.

Of the other tested mutations, the mutations at the Tyr119 and Tyr320 loci had significant effects, while mutations at the Tyr139 locus had modest effects (<10-fold change) on the affinity of salvinorin A for KOR. It appears that the primary mode of interaction at Tyr119 and Tyr320 is via hydrogen bonding: in each case, the majority of the affinity was lost on the mutation from Tyr to Phe; little additional perturbation resulted from the Tyr to Ala mutation. The affinities of U69593 and dynorphin A (1−13) were, in

Table 2: Affinity (K_i, nM) of Salvinorin A, U69593, and Dynorphin A (1−13) Binding to the Wild-Type KOR and Mutants Transiently Expressed in HEK 293 T Cells

			salvinorin A		U69593		dynorphin A (1−13)	
KOR	K_d (nM)[a]	B_{max} (pmol/mg)[a]	K_i (nM)[b]	ratio[c]	K_i (nM)[b]	ratio[c]	K_i (nM)[b]	ratio[c]
wild type	0.25 ± 0.02	5.8 ± 2.0	31.6 ± 6.5		11.7 ± 3.4		1.75 ± 0.35	
Y139A	0.26 ± 0.07	8.3 ± 2.5	53.9 ± 13.9	2	20.6 ± 4.0	2	1.98 ± 0.41	1
Y139F	0.59 ± 0.28	5.0 ± 1.0	193 ± 38	6	101 ± 29	9	13.3 ± 4.6	8
Y312A	0.55 ± 0.10	2.7 ± 0.4	88.6 ± 10.9	3	52.6 ± 11.3	4	1.79 ± 0.28	1
Y312F	0.18 ± 0.03	4.4 ± 0.6	65.1 ± 11.0	2	53.0 ± 12.5	5	1.39 ± 0.22	1
Y313A	0.72 ± 0.18	14.9 ± 0.8	694 ± 106	22	107 ± 32	9	4.10 ± 0.78	2
Y313F	0.26 ± 0.03	7.0 ± 0.1	63.3 ± 15.2	2	37.0 ± 5.0	3	0.93 ± 0.14	1
Y119A	0.19 ± 0.004	1.41 ± 0.02	342 ± 40	11	59.9 ± 2.4	5	6.71 ± 0.89	4
Y119F	0.32 ± 0.09	3.6 ± 0.2	233 ± 66	7	90.7 ± 5.3	8	11.3 ± 4.8	6
Y320A	0.92 ± 0.004	1.3 ± 0.1	380 ± 103	12	195 ± 34	17	3.15 ± 0.82	2
Y320F	0.82 ± 0.33	1.7 ± 0.6	301 ± 75	10	276 ± 88	24	9.68 ± 2.84	6

[a] Saturation binding of ^{3}H-diprenorphine to the wild type and mutants was performed. Data represent, in mean ± SEM form, two or three independent experiments. [b] The affinity constants (K_i) of the different compounds were determined in competition binding assays with ^{3}H-diprenorphine and increasing concentrations of unlabeled compounds. Each value is the mean of three or four independent experiments (see the Experimental Procedures for details). [c] For each compound, the ratio is $K_{i(mutant)}/K_{i(wild-type)}$.

Table 3: Agonist Potency (EC_{50}, nM)[a] and Relative Agonist Efficacy (Normalized E_{max})[a] of Salvinorin A, U69593, and Dynorphin A (1−13) for the Wild-Type KOR and Mutants Transiently Expressed in HEK 293 Cells

	salvinorin A			U69593			dynorphin A (1−13)		
KOR	EC_{50} (nM)	ratio[b]	E_{max} (RFU)	EC_{50} (nM)	ratio[b]	relative E_{max}	EC_{50} (nM)	ratio[b]	relative E_{max}
wild type	45.8 ± 8.1		3232 ± 728	23.6 ± 6.4		1.13 ± 0.19	343 ± 54		1.53 ± 0.26
Y139A	240 ± 44	5	4893 ± 795	140 ± 38	6	1.13 ± 0.29	1044 ± 258	3	1.07 ± 0.15
Y139F	47.0 ± 22.2	1	5265 ± 952	13.3 ± 3.6	1	1.00 ± 0.15	369 ± 98	1	1.17 ± 0.18
Y312A	189 ± 46	4	4667 ± 589	451 ± 225	19	0.93 ± 0.12	416 ± 86	1	0.87 ± 0.18
Y312F	68.3 ± 22.1	1	4308 ± 526	98.0 ± 33.4	4	1.03 ± 0.09	172 ± 39	1	1.30 ± 0.12
Y313A	275 ± 53	6	5124 ± 705	43.9 ± 3.3	2	1.17 ± 0.12	233 ± 44	1	1.23 ± 0.19
Y313F	49.6 ± 15.6	1	5127 ± 747	48.9 ± 12.1	2	0.97 ± 0.42	91 ± 3.4	0.3	1.17 ± 0.52
Y119A	434 ± 163	9	5004 ± 718	358 ± 181	15	0.80 ± 0.26	1290 ± 634	4	0.80 ± 0.26
Y119F	43.5 ± 14.7	1	3880 ± 770	35.9 ± 13.5	2	0.80 ± 0.15	276 ± 99	1	1.03 ± 0.03
Y320A	ND[c]		ND	ND		ND	ND		ND
Y320F	ND		ND	ND		ND	ND		ND

[a] EC_{50} and relative E_{max} were determined from calcium flux assays as described under the Experimental Procedures. The results represent the average of three independent experiments with normalized E_{max} values in mean ± SEM form. [b] For each compound, the ratio is $EC_{50(mutant)}/EC_{50(wild-type)}$. [c] ND = no detectible agonist activity; mutants Y320A and Y320F have no response to salvinorin A, U69593, or dynorphin A (1−13).

general, only modestly affected by the various mutations, with the possible exception of Y320A and Y320F. Interestingly, the single mutation, which had the greatest effect on the affinity of salvinorin A (Y313A) attenuated the affinity of U69593 9-fold and had an insignificant effect on dynorphin A (1−13) affinity (Table 2).

We next determined the agonist potencies and efficacies of salvinorin A, U69593, and dynorphin A (1−13) at wild-type and mutant KORs (Table 3). As expected, the Y313A mutation significantly attenuated the potency of salvinorin A (6-fold), while the Y119A mutation decreased agonist potency 9-fold. Surprisingly, several other mutations attenuated the potency of salvinorin A for activating KORs: Y139A (5-fold) and Y312A (4-fold). These results were intriguing because Y139A and Y312A did not affect binding of salvinorin A to the KOR. The most severe effect was found by mutations Y320A and Y320F. They abolished agonist-induced activation of KOR by all three tested compounds: salvinorin A, U69593, and dynorphin A (1−13). Aside from the Y320 mutations, Y139A (3-fold) and Y119A (4-fold), dynorphin A (1−13) tolerated mutations without losing agonist efficacy. U69593 showed a dramatic loss of potency for activation for the Y312A (19-fold) and Y119A (15-fold) mutations. As with the other compounds, the agonist potency of U69593 was diminished by Y139A 6-fold. In contrast to salvinorin A (6-fold), Y313A only has a 2-fold effect on the ability of U69593 to activate KOR.

Molecular Modeling Predictions. A family of docked solutions was generated for salvinorin A using automated docking techniques (see the Experimental Procedures for details); this family is represented by the model shown in parts A−C of Figure 5. The closest sites of interaction are between salvinorin A and TM1−3, TM6, TM7, and the extracellular loop e2 of the receptor model. In our model, the 2-acetoxy group of salvinorin A is positioned between the e2 loop and the top of TM7 near Tyr313 and the furan ring hydrogen-bonds with Tyr320 in TM7 and Tyr119 in TM2. The 4-methyl ester group is oriented toward the top of TM6. Other models representing different families of docked solutions were also obtained, although they did not account for as many of the observed mutational effects (not shown).

All of the mutated residues in the current model point approximately toward the central cavity, with the exceptions of Leu309 and Ser210, while Tyr312 and Tyr313 are located more remotely near the top of the binding cavity. Table 1 lists the distances between heavy atoms of salvinorin A and nearby amino acid residues in the KOR. Mutations of some of the residues within a distance of 4 Å have been shown by others to affect the binding of conventional KOR ligands. These include Asp138, the putative ammonium-binding residue (*28*); Cys210, the e2 loop disulfide-forming cysteine (*29*); and Ile294, which has been implicated in a SCAM study (*30*). While present in the binding cavity, Tyr139 was not predicted to interact significantly with the docked ligand.

Cys Substitutions Enhance the Binding of 2-Thiosalvinorin B. To more fully elucidate the binding mode of salvinorin A, we examined the binding of a newly synthesized salvinorin A analogue, 2-thiosalvinorin B (**2**) at the wild type and Cys-substituted KOR mutants. We reasoned that Cys substitutions should show enhanced affinity for 2-thiosalvinorin B if the Cys residue was in close proximity to the −SH moiety of 2-thiosalvinorin B. Because the KOR has a single Cys in the binding pocket (Cys315; *30*), we initially characterized C315S. As shown in Table 4, the C315S did not significantly alter the binding of either salvinorin A or 2-thiosalvinorin B. On the basis of the salvinorin A binding model, we constructed several cysteine substitutions in the background of C315S, including Y119C, I294C, E297C, L309C, S310C, and Y313C (Table 4) of which Ile294, Glu297, Leu309, Ser310, and Tyr313 are unique to KORs. As predicted by the salvinorin A binding model, the Y313C mutation *preserved* the affinity of 2-thiosalvinorin B because the −SH group is predicted to be in close proximity to the Cys substitution at the 313 locus in the C315S background. In contrast, the affinity of salvinorin A for the Y313C−C315S double mutant *decreased* by 14.2-fold, presumably because the 2-acetoxy group of salvinorin A cannot form interactions with C313 as effectively or as strongly as 2-thiosalvinorin B. Additionally, I294 and E297, when mutated to Cys, gave rise to significantly enhanced affinities for *both* salvinorin A and 2-thiosalvinorin B.

DISCUSSION

The major finding of this paper is the discovery that a diterpenoid (salvinorin A) utilizes a novel mode for peptidergic GPCR (KOR) binding and activation. We also provide new molecular models that provide reasonable atomic-level

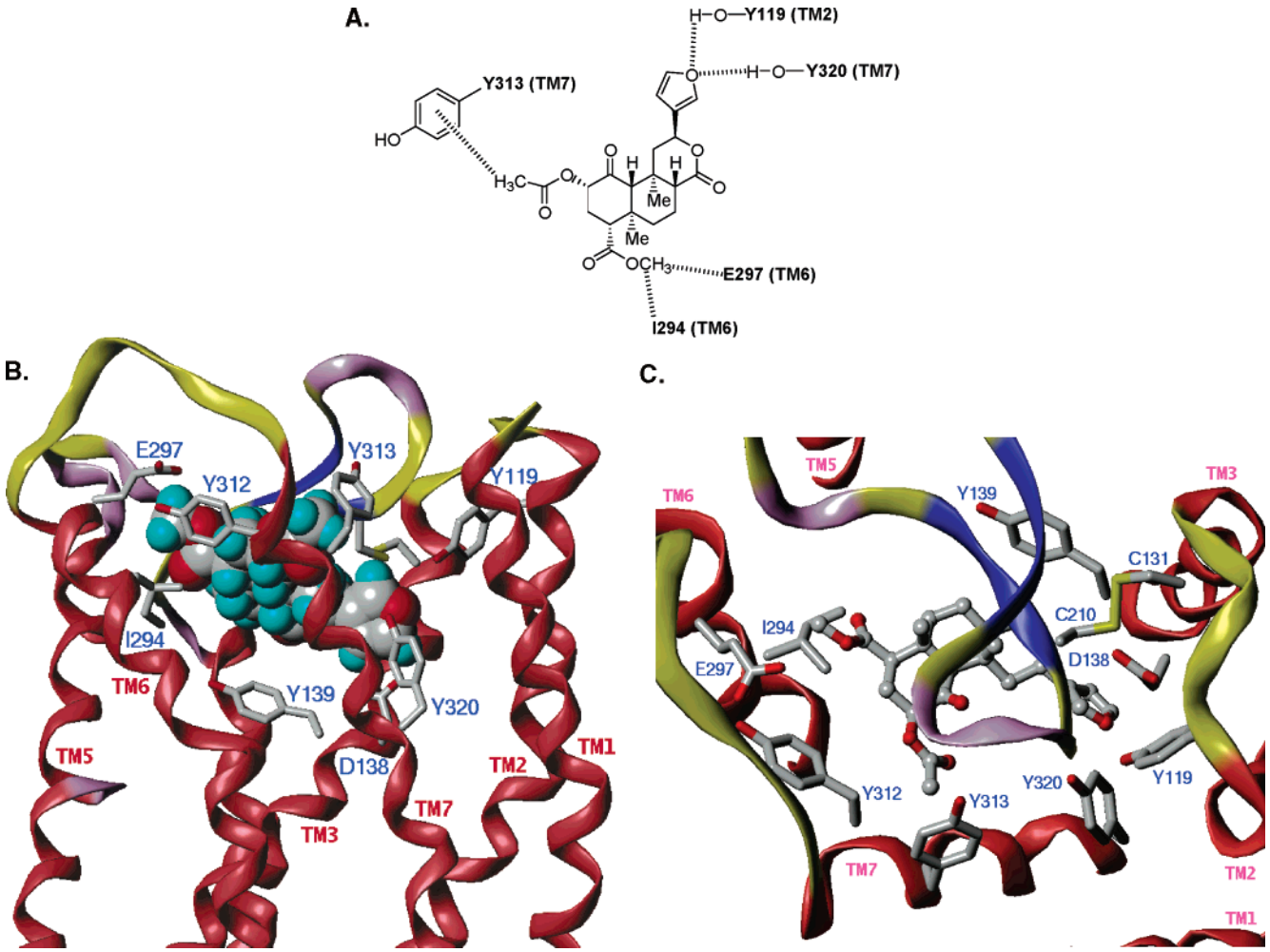

FIGURE 5: Modeling salvinorin A-KOR interactions. (A) Two-dimensional representation of the proposed interactions between salvinorin A and various side chains in the KOR-binding site. (B) Proposed binding mode of salvinorin A in the KOR, looking through the extracellular side of the helical bundle. Tyr313 and Tyr320 in TM7 are nearest to the viewer. The KOR is color-coded based on the assignment of the secondary structure using the Kabsch−Sander (*34*) algorithm (red = helix, blue = β sheet, violet = turn, and yellow = coil). The ligand is rendered as a CPK-style space-filling model. (C) View of the proposed binding model of salvinorin A looking from the extracellular side of the KOR beyond the e2 loop to the binding pocket. For clarity, the intracellular portion of the KOR is not displayed. The ligand is rendered as a ball-and-stick figure, and important nearby residues are rendered as capped stick figures.

Table 4: Effect of Cys-Substitution Mutations[a] on Salvinorin A and 2-Thiosalvinorin B Binding to KORs

	salvinorin A		2-thiosalvinorin B			U69593	
KOR	K_i (nM)[b]	ratio[c]	K_i (nM)[b]	ratio[c]	ratio[d]	K_i (nM)[b]	ratio[c]
wild type	39.6 ± 14.5		157 ± 40		4.0	15.4 ± 3.2	
C315S	37.6 ± 17.6		202 ± 72		5.4	54.3 ± 8.2	
C315S−Y313C	536 ± 66	14.2	219 ± 57	1.1	0.4	59.6 ± 6.5	1.1
C315S−Y119C	178 ± 54	4.7	226 ± 49	1.1	1.3	220 ± 83	4.1
C315S−I294C	6.64 ± 2.71	0.2	43.3 ± 3.8	0.2	6.5	8.26 ± 1.78	0.2
C315S−E297C	4.21 ± 0.89	0.1	36.3 ± 2.1	0.2	8.6	4.88 ± 1.89	0.1
C315S−L309C	20.3 ± 8.9	0.5	92.7 ± 38.8	0.5	4.6	194 ± 97	3.6
C315S−S310C	34.9 ± 8.9	0.9	347 ± 83	1.7	10.0	78.2 ± 21.1	1.4
C315S−Y320C	NA		NA			NA	
C315S−Y66C	66.9 ± 21.2	1.8	214 ± 30	1.1	3.2	180 ± 42	3.3

[a] The double mutants were based on C315 (7.38), which is conserved among the opioid receptor family and is differentially accessible [Xu, et al. (2000) *Biochemistry 39*, 13904−13915]. [b] The affinity constants (K_i) of the different compounds were determined in competition binding assays with ^{3}H-diprenorphine and increasing concentrations of unlabeled compounds. Each value is the mean of two or three independent experiments (see the Experimental Procedures for details). [c] For each compound, the ratio is $K_{i(mutant)}/K_{i(C315S)}$. [d] For each compound, the ratio is $K_{i(2\text{-thiosalvinorin B})}/K_{i(salvinorin A)}$.

explanations for the highly selective binding of a diterpenoid, salvinorin A, to a peptide receptor, the KOR. We also report a novel approach, whereby a designed cysteine-substitution mutagenesis is shown to differentially affect the affinity of salvinorin A and of a salvinorin A derivative with a free sulfhydryl moiety. These results are important because they demonstrate that the exquisitely potent and efficacious interactions of salvinorin A with KORs are due to novel modes of binding within a common three-dimensional space shared by structurally diverse agonists, each of which utilizes

different residues for binding and activating KORs.

Molecular Modeling Considerations. The e2 loop of rhodopsin and most likely all family A GPCRs are connected to a Cys residue near the extracellular side of TM3 by a disulfide bond. In the proposed salvinorin A−KOR binding model, the ligand is docked near the extracellular opening of the binding pocket. One of the most unanticipated features of the rhodopsin structure is that the β hairpin of the e2 loop lies deep in within the helix aggregate and actually comprises part of the retinal-binding site. It has been argued that this feature is unlikely to be conserved in aminergic GPCRs because it may limit access of reversibly bound ligands to the binding site (*31*). However, a recent SCAM investigation of the e2 loop of the dopamine D2 receptor suggests that its structure is rhodopsin-like (*10*). In addition, it has been shown that His319 of TM7 and Asp216 of the e2 loop of the μ-opioid receptor are responsible for the Zn^{2+}-mediated sensitivity of ligand affinity, indicating that these residues are in reasonably close (Cβ−Cβ, 6 Å) proximity (*32*). The distance between the cognate residues, Tyr313 and Glu209, in the rhodopsin-like e2 loop of the KOR models presented here is approximately 8 Å (Cβ−Cβ). These observations, coupled with the demonstration of the necessity of a disulfide bond with the e2 loop, (*29*) imply that the modeled loop structure is accurate.

In the salvinorin A binding model described here, the mutated residues pointed toward a central cavity, although some are clearly less sterically accessible to bound ligands, particularly Tyr312 and Tyr313. Neither Y312A nor Y312F mutations affect the affinity of salvinorin A for the KOR. This is consistent with the proposed model, which indicates only a weak interaction with Tyr312. Interestingly, the Y313A mutation has a large effect on affinity (22-fold), while Y313F has no significant effect. The results of the Y313A and Y313F mutations are consistent with Tyr313 stabilizing the ligand via a hydrophobic-type interaction and with our docked salvinorin A model, which predicts a direct hydrophobic interaction with Tyr313. Although potentially accessible to small molecules, Tyr313 was positioned in a more remote area at the top of the binding cavity interacting with residues in the e2 loop. Tyr313 was previously proposed to provide a hydrogen bond to the 2-acetoxy carbonyl of salvinorin A (*4*) based on docking studies performed using a *de novo* model developed by Mosberg's group (*33*). The current model that is based explicitly on the experimental rhodopsin crystal structure shows a substantial difference in the disposition of Tyr313. The fact that Y313F has no effect on ligand affinity but Y313A reduces affinity by 22-fold has compelled us to modify our original model, wherein we proposed that Tyr313 interacted with salvinorin A primarily via hydrogen-bonding-type interactions. On the basis of our current findings, we propose that a hydrophobic interaction is more likely. In the proposed salvinorin A binding model, the 2-acetoxy group of salvinorin A provides the requisite hydrophobic interaction with Y313, so that salvinorin A retains affinity for the Y313F mutation but loses affinity (22-fold decrease) for the Y313A mutation.

Mutations at other residues also had significant effects on the binding of salvinorin A. Although accessible, the closest Tyr139 side-chain−ligand distance is at least 4 Å away, consistent with the weak effect of either Tyr139 mutation. In our proposed binding model, it is possible for the 17-oxo group to form a weak hydrogen bond with Tyr139; the donor-hydrogen−acceptor (D−H−A) angle is roughly 130° when the ligand carbonyl oxygen−Tyr139 side-chain oxygen distance is 3.0 Å. However, for this hydrogen bond to be formed, the Tyr139 χ_1 torsion angle must assume values that give rise to higher energy eclipsed conformations, consistent with the modest 6-fold increase in the K_i observed for the Y139F mutation. The Y139A mutation (only 2-fold decrease in affinity) suggests that an amino acid side chain that is a small hydrophobic group, rather than a large hydrophobic group, is beneficial when the interaction takes place with a hydrophilic group on the ligand. Both mutations of Tyr320 result in the loss of affinity for salvinorin A by about 10-fold, suggesting hydrogen-bond involvement. Our proposed model interacts with Tyr320 via hydrogen bonding with the furanyl substituent of salvinorin A. However, this hydrogen bond is expected to be somewhat weaker than a normal hydrogen bond because the accepting lone-pair electrons of the oxygen atom are partially delocalized in the furan ring. The interatomic distance between the furan oxygen atom in salvinorin A and the Tyr320 side chain oxygen is 3.0 Å. Mutation of Tyr119 to either Phe or Ala decreases the affinity of salvinorin A for the KOR but to a somewhat lesser extent than for the analogous Tyr320 mutations, again indicating that hydrogen-bond interactions are involved. As with Tyr320, our proposed salvinorin A model interacts with Tyr119 via hydrogen bonding with the furanyl substituent of the ligand. It places the furan ring oxygen atom somewhat farther away from Tyr119 (3.6 Å) than from Tyr320 (3.0 Å), potentially explaining the slightly greater decrease in binding affinity for the Tyr320 mutation when compared to the analogous Tyr119 mutation.

To further explore the interactions of the salvinorins with the KOR, we employed a novel approach, whereby we combined cysteine-substitution mutagenesis with an evaluation of the binding of 2-thiosalvinorin B and salvinorin A. We reasoned that, if residues mutated to Cys were in close proximity to the thiol of 2-thiosalvinorin B, there should be an enhancement (or at least a retention) of the affinity of 2-thiolsalvinorin B for the KOR, while the affinity for salvinorin A would likely decrease. An inspection of the salvinorin A binding model disclosed that Tyr313, when mutated to Cys, would yield a Cys residue that is predicted to be in close proximity to the free thiol of 2-thiosalvinorin B. In addition, mutating other nearby residues in a similar fashion would produce Cys residues nearer to other positions on the salvinorin molecule. If our proposed model is correct, mutations at these non-Tyr313 positions should affect the binding of salvinorin A and 2-thiosalvinorin B roughly equally, because salvinorin A and 2-thiosalvinorin B differ only at the 2 position. The results of these experiments are presented in Table 4 and agree with the predictions.

In our model of the KOR, the side chain of Cys315 is located in the interface between helices TM6 and TM7; therefore, it is not surprising that the mutation C315S did not result in a statistically significant change in the binding affinity for either salvinorin A or 2-thiosalvinorin B (Table 4). The most significant result from the Cys-substitution mutation studies is that the double-mutant C315S−Y313C KOR has 14.2-fold less affinity for salvinorin A than does the C315S single-mutant KOR, whereas the affinity of the double-mutant KOR for 2-thiosalvinorin B is largely unaf-

fected compared to the single-mutant C315S KOR. This would suggest that it is indeed the 2 position of the salvinorins that interact with Tyr313, because an SH-acetoxy interaction (in the case of salvinorin A) would be very weak and would increase the K_i significantly, whereas an SH−SH interaction (in the case of 2-thiosalvinorin B) would be stronger because of hydrophobic interactions and/or disulfide bond formation and would allow the double mutant to retain affinity for 2-thiosalvinorin B. We believe disulfide bond formation is unlikely because preliminary studies have demonstrated that prolonged exposure to 2-thiosalvinorin B does not lead to an irreversible loss of binding (data not shown). Our proposed model also positions the 4-methyl ester group in very close proximity to both Ile294 and Glu297. The double mutations C315S−I294C and C315S−E297C each affect both salvinorins roughly equally, increasing the affinity of both by 5−10-fold. Because both salvinorins are affected equally, it is probable that a substituent that is common to both (the 4-methyl ester group in this case, not the 2-position substituent) is interacting at Ile294 and Glu297. The nature of these interactions is unclear, because both hydrophobic and hydrophilic hydrogen-bond acceptor regions are present. However, visual inspection of space-filling models reveals that the terminal methyl of the ester group at the 4 position of salvinorin A can interact with hydrophobic portions of the Ile294 and Glu297 side chains. The lipophilic interaction between I294 and E297 and the 4 position is shown fairly clearly in Figures 5 and 6. Mutation of either of these residues to Cys would retain some hydrophobic interaction potential and perhaps more importantly would remove some of the steric bulk in the region, allowing the 4 position to more effectively associate with the side chains at positions 294 and 297. The double mutations involving Leu309 and Ser310 did not significantly alter the binding affinity of either salvinorin, and this is consistent with our proposed model complex in that these residues are not part of the ligand-binding site. No data could be obtained for the C315S−Y320C double mutation, because this mutation was inactive. 2-Thiolsalvinorin B can be docked into the KOR in an orientation similar to the proposed model for salvinorin A (see Figure 6).

When these findings are taken together, they support a mode of binding whereby salvinorin A and 2-thiosalvinorin B interact with the KOR via residues that are not utilized by conventional KOR peptide and non-peptide agonists [e.g., dynorphin A (1−13) and U69593, respectively]. These residues probably line a putative binding pocket that overlaps in three-dimensional space with that used by nitrogenous KOR agonists. Thus, compounds such as U69593 are predicted to bind in approximately the same three-dimensional space but do so by utilizing different residues. It is likely that the extraordinary selectivity and potency for KORs of salvinorin A are due to the fact that it uses these "unusual" and generally nonconserved residues for ligand binding. Residues with which our proposed model interacts (namely, Ile294, Glu297, and Tyr313) are unique to the KOR. In addition, because there is no relatively strong salt bridge anchoring salvinorin A into the binding pocket and because there are many hydrogen-bonding and lipophilic interaction sites within the pocket, it would not be unexpected for the KOR to recognize salvinorin A via more than one binding mode. It is possible that these various models, taken together, could collectively give rise to the observed affinity and/or activation of the KOR and that no individual model would be totally responsible for the observed effects. It is likely that studies with additional salvinorin A analogues will help us to further refine the binding mode of salvinorin A and related compounds.

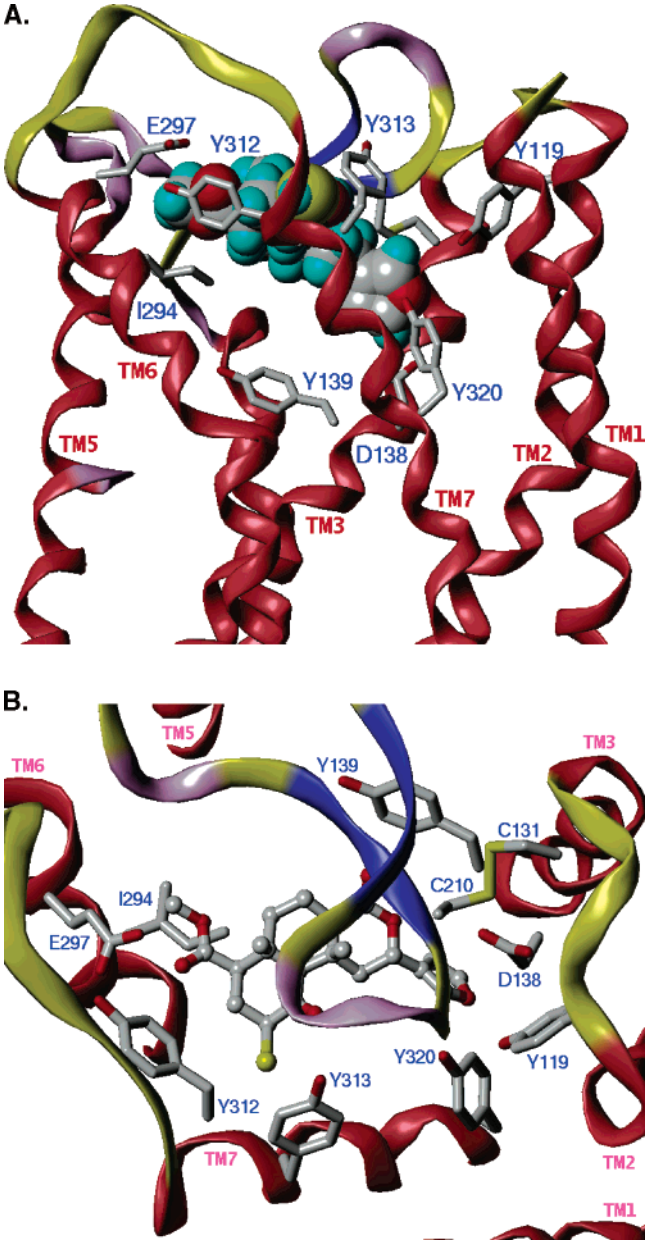

FIGURE 6: Proposed binding modes of 2-thiosalvinorin B in the KOR. (A) Proposed binding modes of 2-thiosalvinorin B in the KOR, looking through the extracellular side of the helical bundle. The KOR is color-coded based on the assignment of the secondary structure using the Kabsch-Sander (*34*) algorithm (red = helix, blue = β sheet, violet = turn, and yellow = coil). A view of the proposed binding model of 2-thiosalvinorin B looking from the extracellular side of the KOR beyond the e2 loop to the binding pocket.

REFERENCES

1. Valdes, L. J., Butler, W. M., Hatfield, G. M., Paul, A. G., and Koreeda, M (1984) Divinorin A: A psychotropic terpenoid and divnorin B from the hallucinogenic Mexican mint *Salvia divinorum*, *J. Org. Chem. 49*, 4716−7720.
2. Valdes, L. J., III, Diaz, J. L., and Paul, A. G. (1983) Ethnopharmacology of ska Maria Pastora (*Salvia divinorum*, Epling and Jativa-M.), *J. Ethnopharmacol. 7*, 287−312.

3. Siebert, D. J. (1994) *Salvia divinorum* and salvinorin A: New pharmacologic finding, *J. Ethnopharmacol. 43*, 53−56.
4. Roth, B. L., Baner, K., Westkaemper, R., Siebert, D., Rice, K. C., Steinberg, S., Ernsberger, P., and Rothman, R. B. (2002) Salvinorin A: A potent naturally occurring nonnitrogenous κ opioid selective agonist, *Proc. Natl. Acad. Sci. U.S.A. 99*, 11934−11939.
5. Sheffler, D. J., and Roth, B. L. (2003) Salvinorin A: The "magic mint" hallucinogen finds a molecular target in the κ opioid receptor, *Trends Pharmacol. Sci. 24*, 107−109.
6. Chavkin, C., Sud, S., Jin, W., Steward, J., Zjawiony, J. K., Siebert, D., Toth, B. A., Hufeisen, S. J., and Roth, B. L. (2004) Salvinorin A, an active component of the hallucinogenic sage *Salvia divinorum*, is a highly efficacious κ opioid receptor agonist: Structural and functional considerations, *J. Pharmacol. Exp. Ther. 308*.
7. Wang, Y., Tang, K., Inan, S., Siebert, D. J., Holzgrabe, U., Lee, D. Y., Huang, P., Li, J. G., Cowan, A., and Liu-Chen, L. Y. (2004) Comparison of pharmacological activities of three distinct κ ligands (salvinorin A, TRK-820, and 3FLB) on κ opioid receptors *in vitro* and their antipruritic and antinociceptive activities *in vivo*, *J. Pharmacol. Exp. Ther. 308*.
8. Ballesteros, J. A., Shi, L., and Javitch, J. A. (2001) Structural mimicry in G protein-coupled receptors: Implications of the high-resolution structure of rhodopsin for structure−function analysis of rhodopsin-like receptors, *Mol. Pharmacol. 60*, 1−19.
9. Shapiro, D. A., Kristiansen, K., Weiner, D. M., Kroeze, W. K., and Roth, B. L. (2002) Evidence for a model of agonist-induced activation of 5-HT2A serotonin receptors which involves the disruption of a strong ionic interaction between helices 3 and 6, *J. Biol. Chem. 18*, 18.
10. Shi, L., and Javitch, J. A. (2004) The second extracellular loop of the dopamine D2 receptor lines the binding-site crevice, *Proc. Natl. Acad. Sci. U.S.A. 101*, 440−445.
11. Shapiro, D. A., Kristiansen, K., Kroeze, W. K., and Roth, B. L. (2000) Differential modes of agonist binding to 5-hydroxytryptamine-(2A) serotonin receptors revealed by mutation and molecular modeling of conserved residues in transmembrane region 5, *Mol. Pharmacol. 58*, 877−886.
12. Kristiansen, K. (2004) Molecular mechanisms of ligand binding, signaling, and regulation within the superfamily of G-protein-coupled receptors: Molecular modeling and mutagenesis approaches to receptor structure and function, *Pharmacol. Ther. 103*, 21−80.
13. Stewart, D. J. Doctoral Dissertation, University of Mississippi, February 25, 2005.
14. Chavkin, C., Sud, S., Jin, W., Stewart, J., Zjawiony, J. K., Siebert, D. J., Toth, B. A., Hufeisen, S. J., and Roth, B. L. (2004) Salvinorin A, an active component of the hallucinogenic sage *Salvia divinorum* is a highly efficacious κ-opioid receptor agonist: Structural and functional considerations, *J. Pharmacol. Exp. Ther. 308*, 1197−1203.
15. Westkaemper, R. B., and Glennon, R. A. (2002) Application of ligand SAR, receptor modeling, and receptor mutagenesis to the discovery and development of a new class of 5-HT(2A) ligands, *Curr. Top. Med. Chem. 2*, 575−598.
16. Baldwin, J. M., Schertler, G. F., and Unger, V. M. (1997) An α-carbon template for the transmembrane helices in the rhodopsin family of G-protein-coupled receptors, *J. Mol. Biol. 272*, 144−164.
17. Palczewski, K., Kumasaka, T., Hori, T., Behnke, C. A., Motoshima, H., Fox, B. A., Le Trong, I., Teller, D. C., Okada, T., Stenkamp, R. E., Yamamoto, M., and Miyano, M (2000) Crystal structure of rhodopsin: A G protein-coupled receptor [see comments], *Science 289*, 739−745.
18. Bower, M. J., Cohen, F. E., and Dunbrack, R. L., Jr. (1997) Prediction of protein side-chain rotamers from a backbone-dependent rotamer library: A new homology modeling tool, *J. Mol. Biol. 267*, 1268−1282.
19. Ronsisvalle, G., Pasquinucci, L., Pappalardo, M. S., Vittorio, F., Fronza, G., Romagnoli, C., Pistacchio, E., Spampinato, S., and Ferri, S. (1993) Non-peptide ligands for opioid receptors. Design of κ-specific agonists, *J. Med. Chem. 36*, 1860−1865.
20. Lavecchia, A., Greco, G., Novellino, E., Vittorio, F., and Ronsisvalle, G. (2000) Modeling of κ-opioid receptor/agonists interactions using pharmacophore-based and docking simulations, *J. Med. Chem. 43*, 2124−2134.
21. Mansour, A., Taylor, L. P., Fine, J. L., Thompson, R. C., Hoversten, M. T., Mosberg, H. I., Watson, S. J., and Akil, H. (1997) Key residues defining the μ-opioid receptor binding pocket: A site-directed mutagenesis study, *J. Neurochem. 68*, 344−353.
22. Sharma, S. K., Jones, R. M., Metzger, T. G., Ferguson, D. M., and Portoghese, P. S. (2001) Transformation of a κ-opioid receptor antagonist to a κ-agonist by transfer of a guanidinium group from the 5′- to 6′-position of naltrindole, *J. Med. Chem. 44*, 2073−2079.
23. Larson, D. L., Jones, R. M., Hjorth, S. A., Schwartz, T. W., and Portoghese, P. S. (2000) Binding of norbinaltorphimine (norBNI) congeners to wild-type and mutant μ and κ opioid receptors: Molecular recognition loci for the pharmacophore and address components of κ antagonists, *J. Med. Chem. 43*, 1573−1576.
24. Meng, F., Hoversten, M. T., Thompson, R. C., Taylor, L., Watson, S. J., and Akil, H. (1995) A chimeric study of the molecular basis of affinity and selectivity of the κ and the δ opioid receptors. Potential role of extracellular domains, *J. Biol. Chem. 270*, 12730−12736.
25. Watson, B., Meng, F., and Akil, H. (1996) A chimeric analysis of the opioid receptor domains critical for the binding selectivity of μ opioid ligands, *Neurobiol. Dis. 3*, 87−96.
26. Jones, G., and Willett, P (1995) Docking small-molecule ligands into active sites, *Curr. Opin. Biotechnol. 6*, 652−656.
27. Jones, G., Willett. P., Glen, R. C., Leach, A. R., and Taylor, R. (1997) Development and validation of a genetic algorithm for flexible docking, *J. Mol. Biol. 267*, 727−748.
28. Kong, H. Y., Raynor, K., and Reisine, T. (1994) Amino acids in the cloned κ receptor that are necessary for the high affinity agonist binding but not antagonist binding, *Regul. Pept. 54*, 155−156.
29. Ott, D., Frischknecht, R., and Pluckthun, A. (2004) Construction and characterization of a κ opioid receptor devoid of all free cysteines, *Protein Eng. Des. Sel. 17*, 37−48.
30. Xu, W., Li, J., Chen, C., Huang, P., Weinstein, H., Javitch, J. A., Shi, L., de Riel, J. K., and Liu-Chen, L. Y. (2001) Comparison of the amino acid residues in the sixth transmembrane domains accessible in the binding-site crevices of μ, δ, and κ opioid receptors, *Biochemistry 40*, 8018−8029.
31. Bourne, H. R., and Meng, E. C. (2000) Structure. Rhodopsin sees the light, *Science 289*, 733−734.
32. Fowler, C. B., Pogozheva, I. D., LeVine, H., III, and Mosberg, H. I. (2004) Refinement of a homology model of the μ-opioid receptor using distance constraints from intrinsic and engineered zinc-binding sites, *Biochemistry 43*, 8700−8710.
33. Pogozheva, I. D., Lomize, A. L., and Mosberg, H. I. (1998) Opioid receptor three-dimensional structures from distance geometry calculations with hydrogen bonding constraints, *Biophys. J. 75*, 612−634.
34. Kabsch, W., and Sander, C. (1983) Dictionary of protein secondary structure: Pattern recognition of hydrogen-bonded and geometrical features, *Biopolymers 22*, 2577−2637.

BI050490D